SUPPORTING INFORMATION

A Binuclear Thorium Complexes with Th-O-Th Unit

Yifei He,[a, b#] Yicheng Huang,[c#] Kang Liu,[d#] Congzhi Wang,[b] Xiangyu Liu,[a*] Liyong Yuan,[b] Jipan Yu,[b*] Yan Guo[a, b*], Weiqun Shi[b, c*]

[a] State Key Laboratory of High-efficiency Utilization of Coal and Green Chemical Engineering, College of Chemistry and Chemical Engineering, Ningxia University, Yinchuan 750021, China.

[b] Laboratory of Nuclear Energy Chemistry, Institute of High Energy Physics, Chinese Academy of Sciences, Beijing 100049, China.

[c] School of Mechanical Engineering, Shanghai Jiao Tong University, Shanghai 200240, China.

[d] School of Science, China University of Geosciences, Beijing 100083, China.

Table of Contents

Experimental

Synthesis of 1. [Trapen^{TMS}(Li)$_3$] (1.13 g, 2.0 mmol) was dissolved in THF (15 mL), and the solution was slowly added to the pre-cooled (-30 ^{o}C) THF solution containing $ThCl_4(DME)_2$. The mixture was warmed to room temperature and stirred for further 12 h. All volatiles were removed under vacuum. Toluene (25 mL) was added and the resulting pale-yellow suspension was filtered to remove white solids. The solvent was removed in vacuum and colorless crystals were grown from a saturated solution of toluene at -30 ^{o}C. Yield :1.14 g, 70%. ^{1}H NMR (500 MHz, C_6D_6, 298 K): δ (ppm) 7.14 (t, J = 7.7 Hz, 3H), 7.05 (m, 6H), 6.86 (t, J = 7.7 Hz, 3H), 4.42 (d, J = 11.8 Hz, 3H), 2.44 (d, J = 11.8 Hz, 3H), 0.13 (s, 27H). ^{13}C NMR (125 MHz, C_6D_6, 298 K): δ (ppm) 148.16 (s, Ar*C*), 132.78 (s, Ar*C*), 130.38 (s, Ar*C*), 129.99 (s, Ar*C*), 128.88 (s, Ar*C*), 122.22 (s, Ar*C*), 59.47 (s, N*C*H$_2$), 0.90 (s, NSi(*C*H$_3$)$_3$). ^{29}Si NMR (99 MHz, C_6D_6, 298 K): δ (ppm) -50.00. Anal. Calcd for $C_{30}H_{45}ClN_4Si_3Th$: C, 44.30; H, 5.58; N, 6.65. Found: C, 44.80; H, 5.39; N, 6.89. FT-IR ν/cm^{-1} (KBr): 2949(m), 1597(m), 1472(s), 1441(m), 1231(s), 1034(m), 939(m), 908(s), 840(vs), 798(s), 746(s), 705(m), 475(m).

Synthesis of 2. THF (10 mL) was added to a mixture of **1** and NaN_3 (71.5 mg, 1.1 mmol) at -30 ^{o}C. The mixture was warmed to room temperature

with stirring over 12 h. Volatiles were removed under vacuum and the solid resulting was extracted into toluene (25 mL). The solution was filtered and concentrated to 5 mL, slowly evaporated and cooled to -30 °C to obtain a colorless crystal. Yield : 451 mg, 55%. ^{1}H NMR (500 MHz, C_6D_6, 298 K): δ (ppm) 7.15 (t, J = 7.6 Hz, 6H), 7.05 (t, J = 8.0 Hz, 12H), 6.86 (t, J = 8.0 Hz, 6H), 4.43 (d, J = 11.7 Hz, 6H), 2.44 (d, J = 11.7 Hz, 6H), 0.10 (s, 54H). ^{13}C NMR (125 MHz, C_6D_6, 298 K): δ (ppm) 148.22 (s, Ar*C*), 132.80 (s, Ar*C*), 130.45 (s, Ar*C*), 129.34 (s, Ar*C*), 128.99 (s, Ar*C*), 122.71 (s, Ar*C*), 58.76 (s, N*C*H_2), 1.12 (s, NSi(*C*H_3)$_3$). ^{29}Si NMR (99 MHz, C_6D_6, 298 K): δ (ppm) -5.23. Anal. Calcd for $C_{64}H_{98}ON_{14}Si_6Th_2$: C, 44.90; H, 5.77; N, 11.45. Found: C, 44.14; H, 5.44; N, 12.12. FT-IR ν/cm^{-1} (KBr): 2947(m), 2844(m), 2127(vs), 2086(s), 1472(m), 1446(m), 1237(s), 1032(m), 904(s), 833(vs), 797(s), 746(s), 710(m), 674(m), 591(m), 471(s).

Synthesis of 3. Complex **2** (410 mg, 0.25 mmol) was dissolved in THF (20 mL) and cooled to -30 °C. KC_8 (81 mg, 0.6 mmol) was slowly added to the solution and quickly turned black. The resultant mixture was stirred at room temperature for another 12 h. All volatiles were removed under vacuum. Toluene (25 mL) was added and the resulting pale-yellow suspension was filtered to remove white solids. The yellow filtrate was concentrated to 0.5 mL and cooled to -30 °C to obtain a colorless crystal 161 mg. Yield : 42%. ^{1}H NMR (500 MHz, C_6D_6, 298 K): δ (ppm) 7.32 (t,

J = 6.8 Hz, 6H), 7.16 (m, 12H), 7.01 (t, *J* = 7.2 Hz, 6H), 4.37 (d, *J* = 12.4 Hz, 6H), 2.41 (d, *J* = 11.6 Hz, 6H), 0.14 (m, 54H). ^{13}C NMR (125 MHz, C_6D_6, 298 K): δ (ppm) 149.09 (s, Ar*C*), 133.02 (s, Ar*C*), 130.82 (s, Ar*C*), 129.34 (s, Ar*C*), 128.06 (s, Ar*C*), 122.41 (s, Ar*C*), 59.94 (s, N*C*H_2), 1.40 (s, NSi(*C*H_3)$_3$). Anal. Calcd for $C_{74}H_{106}N_8OSi_6Th_2$: C, 50.64; H, 6.14; N, 7.18. Found: C, 50.21; H, 5.93; N, 7.55. FT-IR *v*/cm^{-1} (KBr): 3057(w), 3007(w), 2940(s), 2894(m), 2852(m), 2093(w), 2045(w), 1591(m), 1472(s), 1443(s),1370(w), 1240(vs), 1064(w), 1040(m), 944(s), 911(m), 843(vs), 797(m), 747(m), 709(m), 681(m), 621(w), 595(m), 556(m), 523(m), 477(s).

NMR spectra

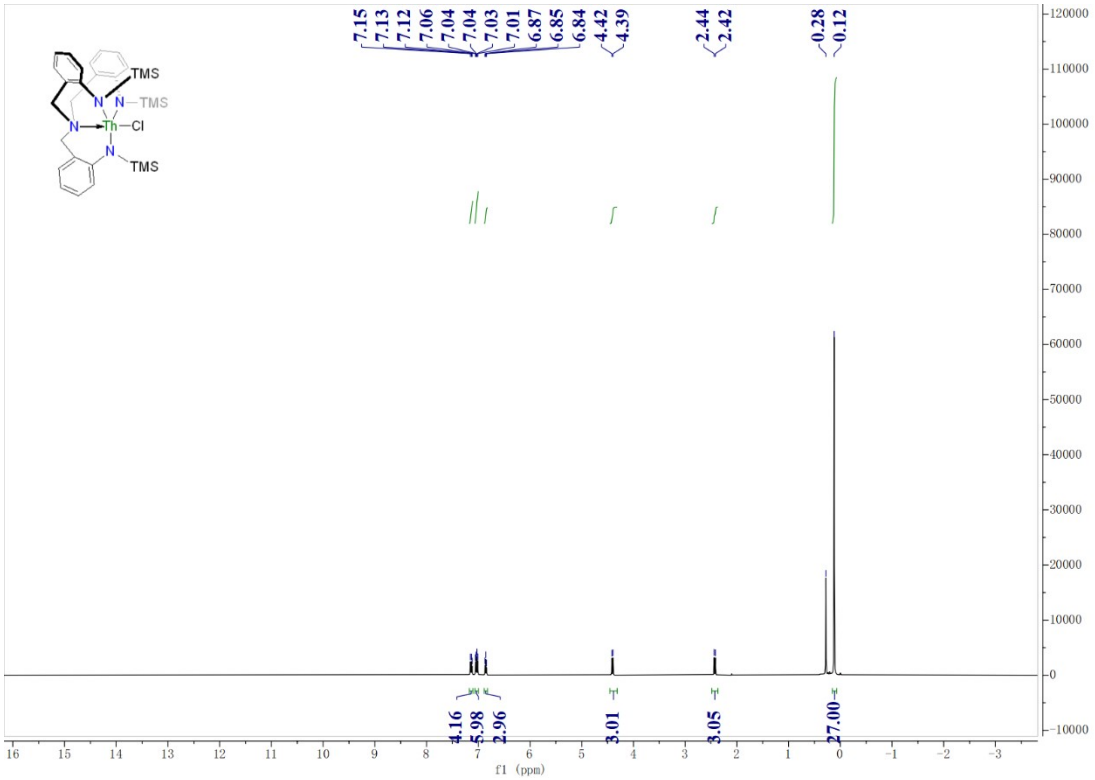

Figure S1. ^{1}H NMR spectrum of Complex **1** in C_6D_6 at 25℃.

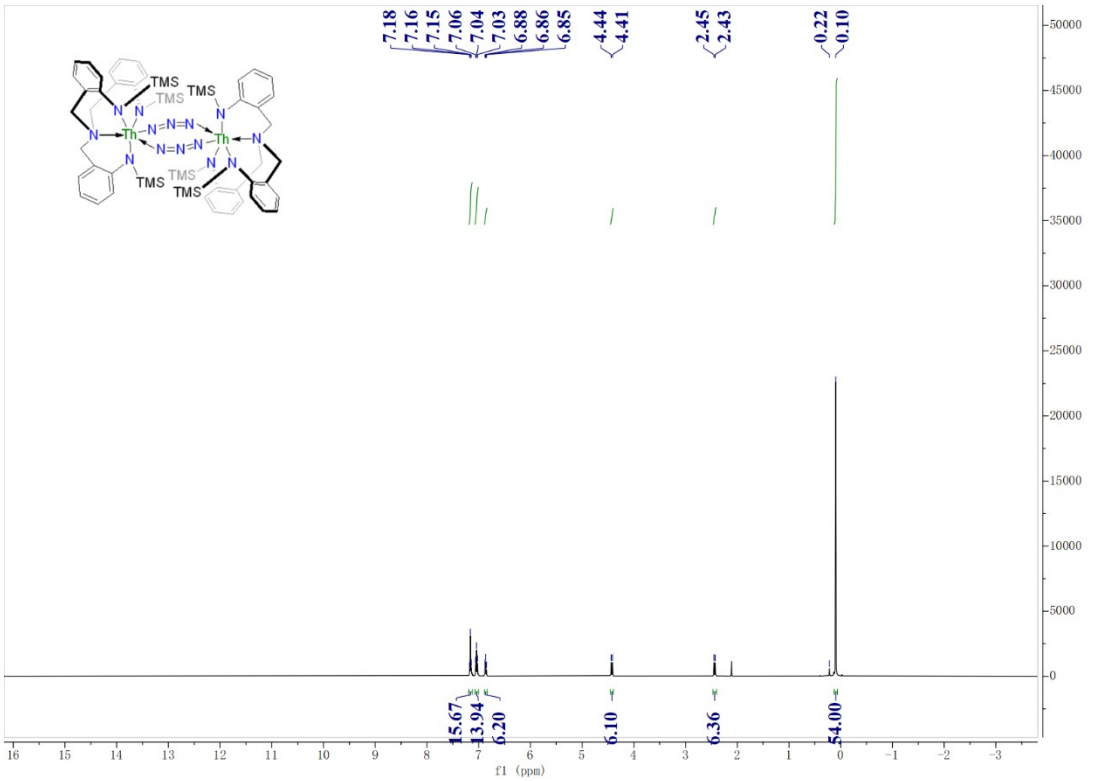

Figure S2. ^{1}H NMR spectrum of Complex **2** in C_6D_6 at 25℃.

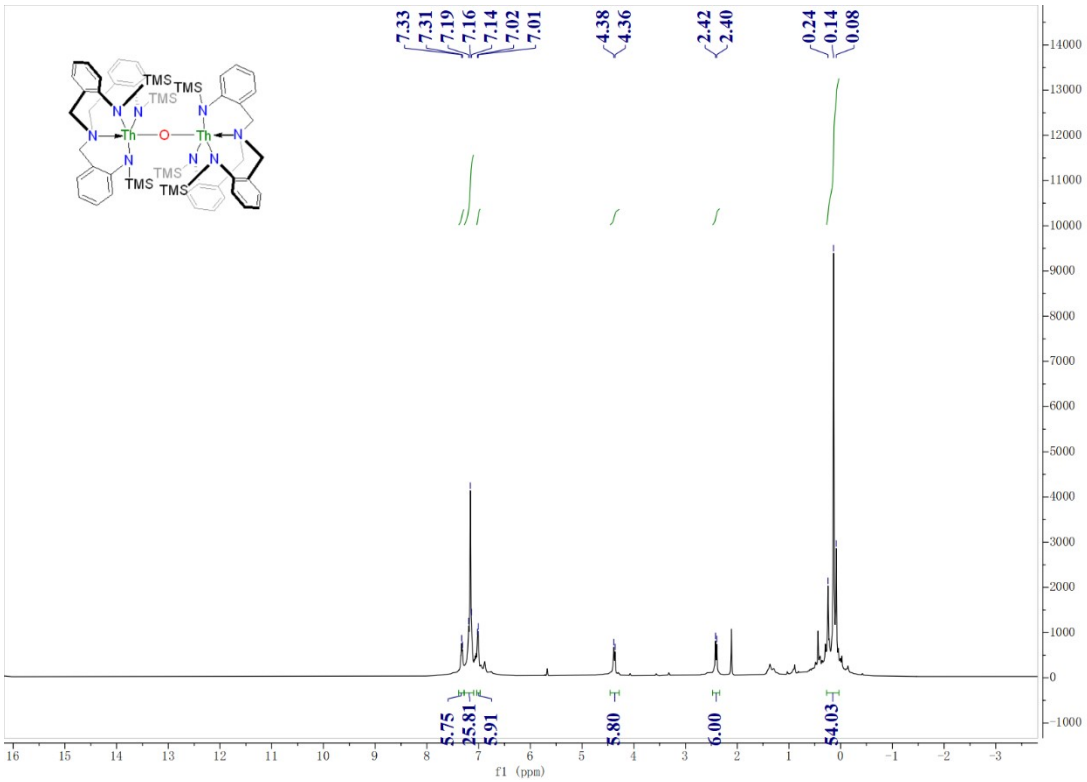

Figure S3. ^{1}H NMR spectrum of Complex **3** in C_6D_6 at 25℃.

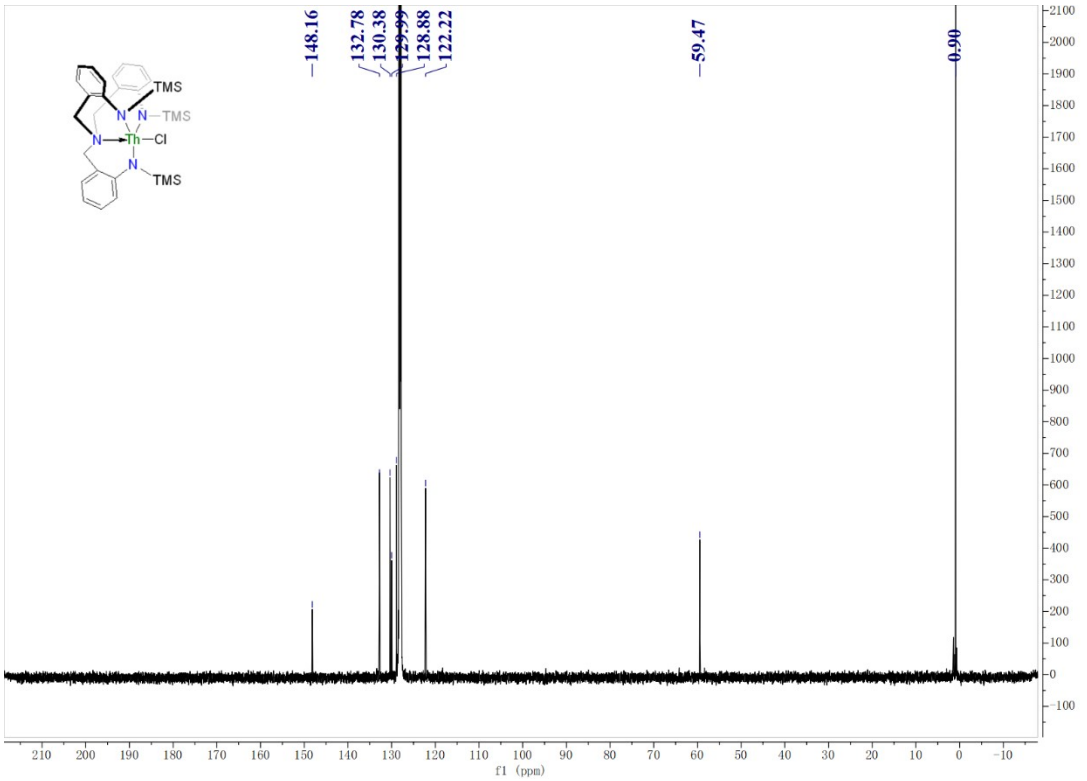

Figure S4. ^{13}C NMR spectrum of Complex **1** in C_6D_6 at 25℃.

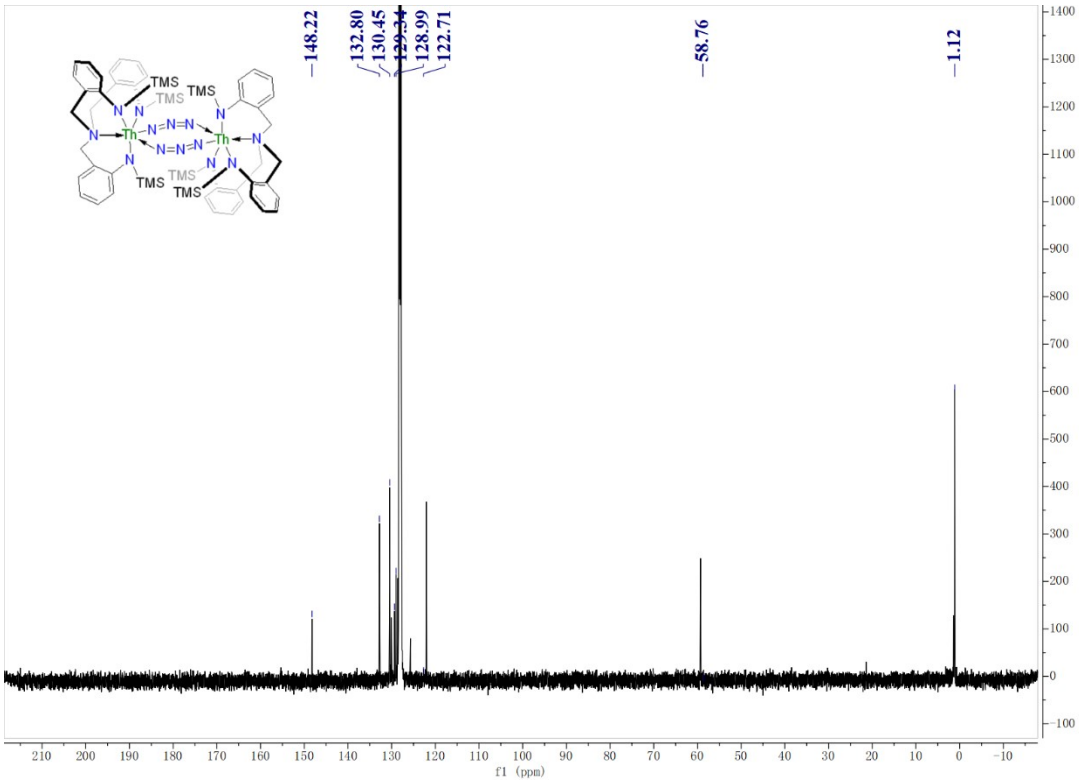

Figure S5. ^{13}C NMR spectrum of Complex **2** in C_6D_6 at 25°C.

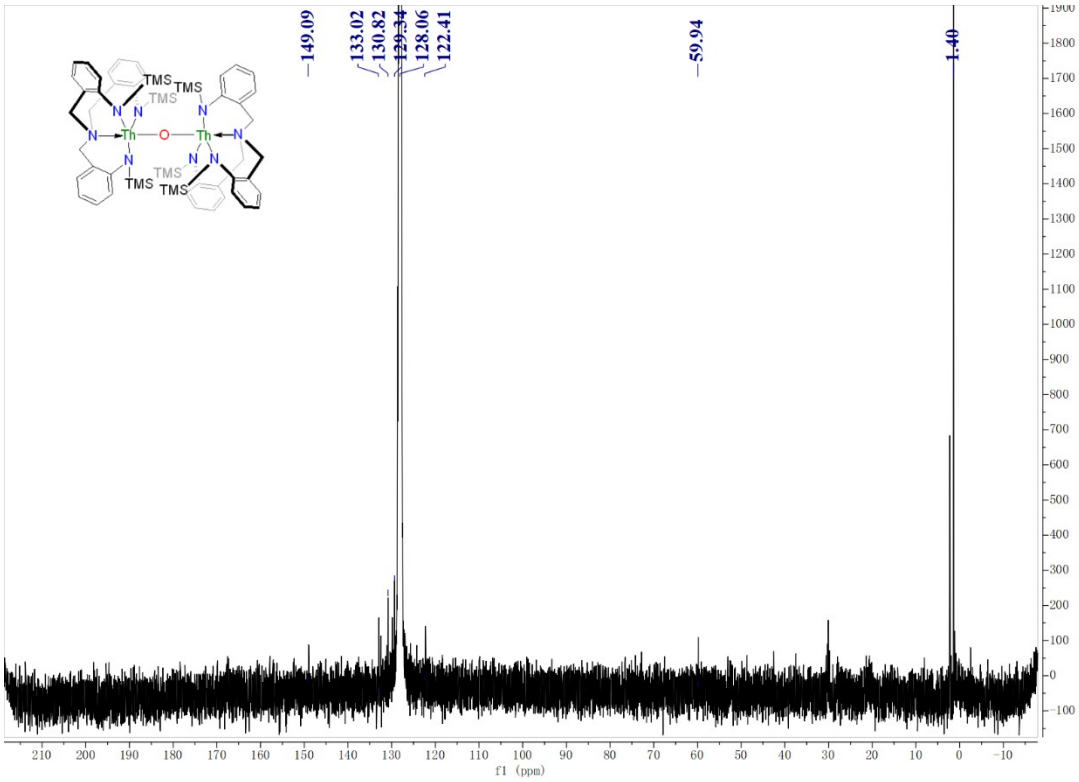

Figure S6. ^{13}C NMR spectrum of Complex **3** in C_6D_6 at 25°C.

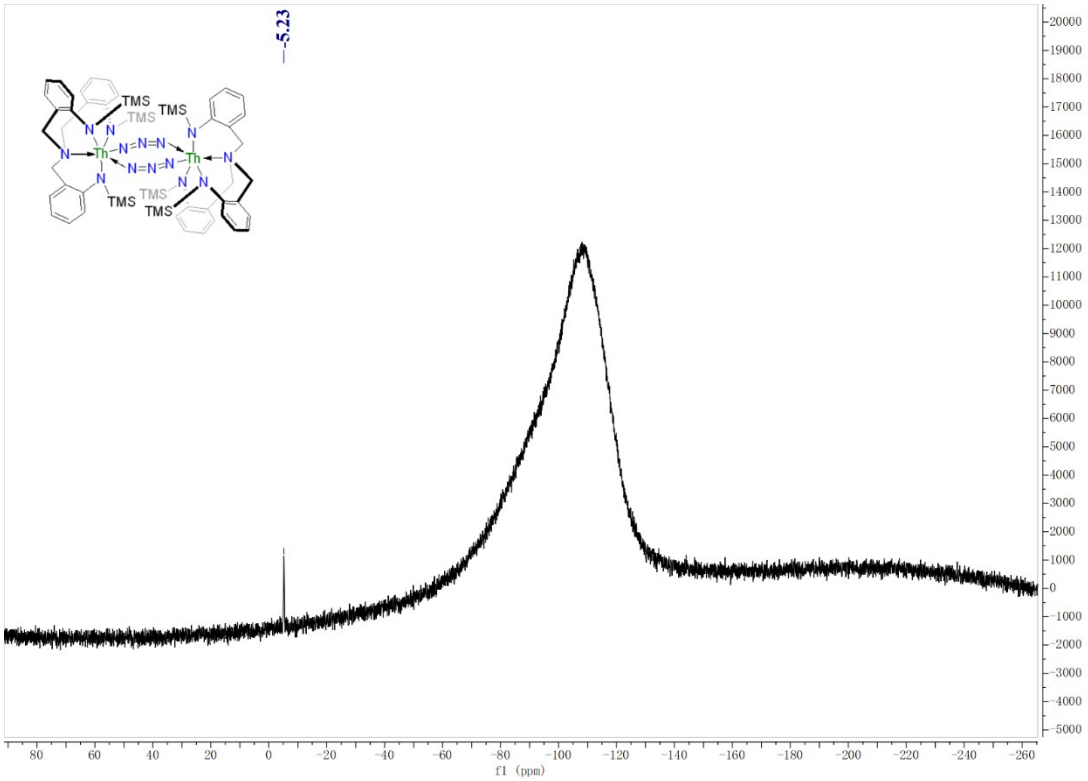

Figure S7. ^{29}Si NMR spectrum of Complex **2** in C_6D_6 at 25℃.

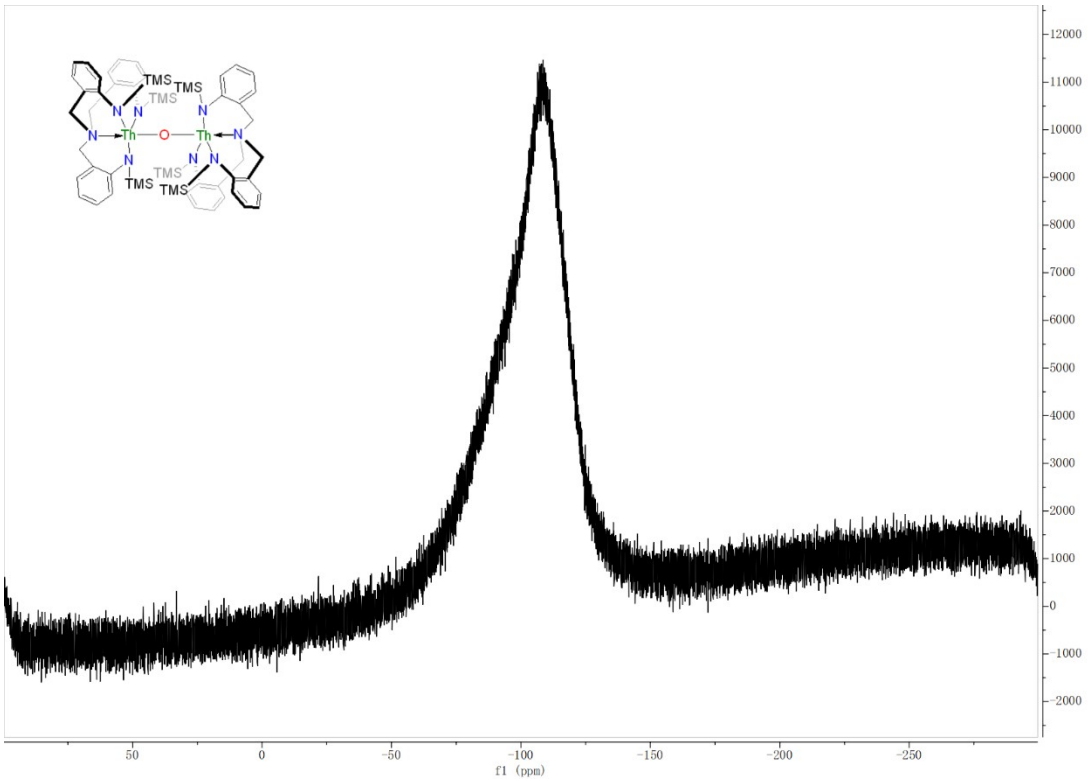

Figure S8. ^{29}Si NMR spectrum of Complex **3** in C_6D_6 at 25℃.

IR spectra

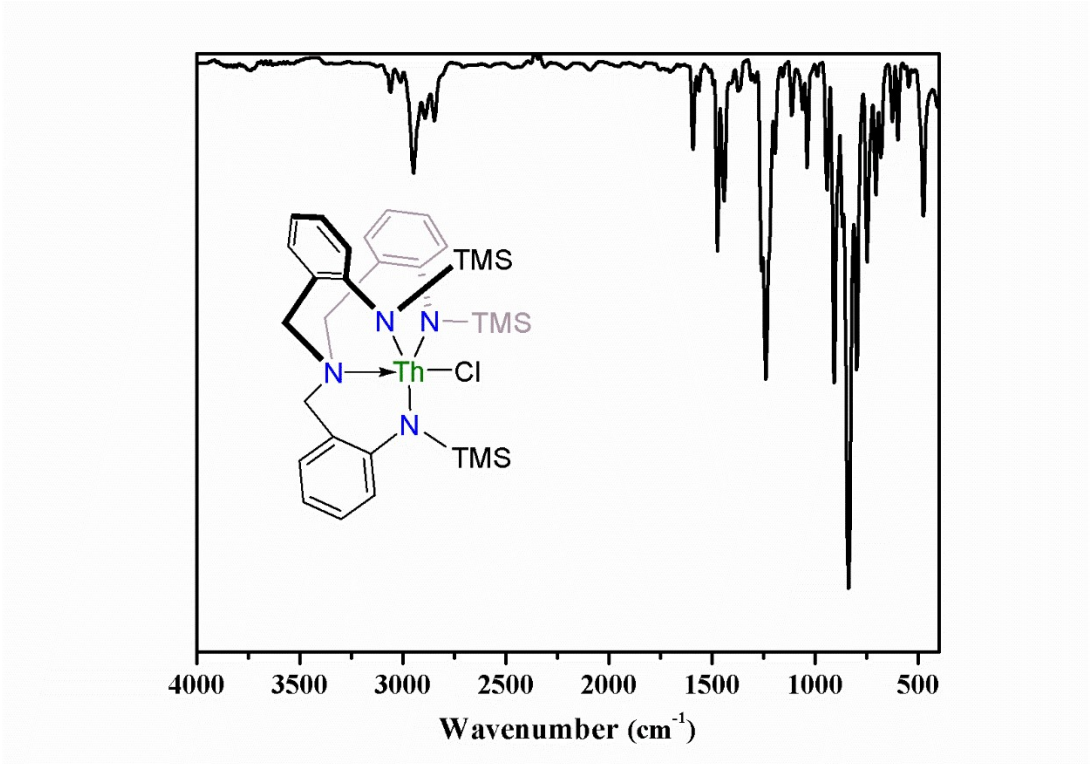

Figure S9. IR spectrum of Complex **1.**

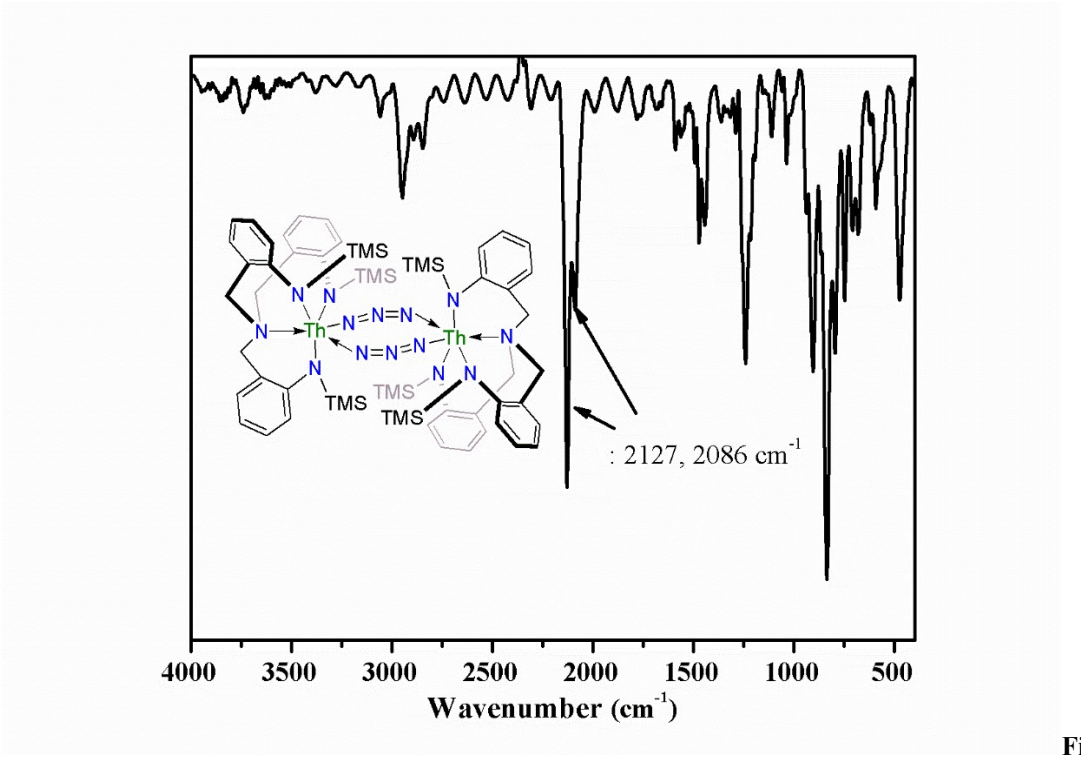

Figure S10. IR spectrum of Complex **2**.

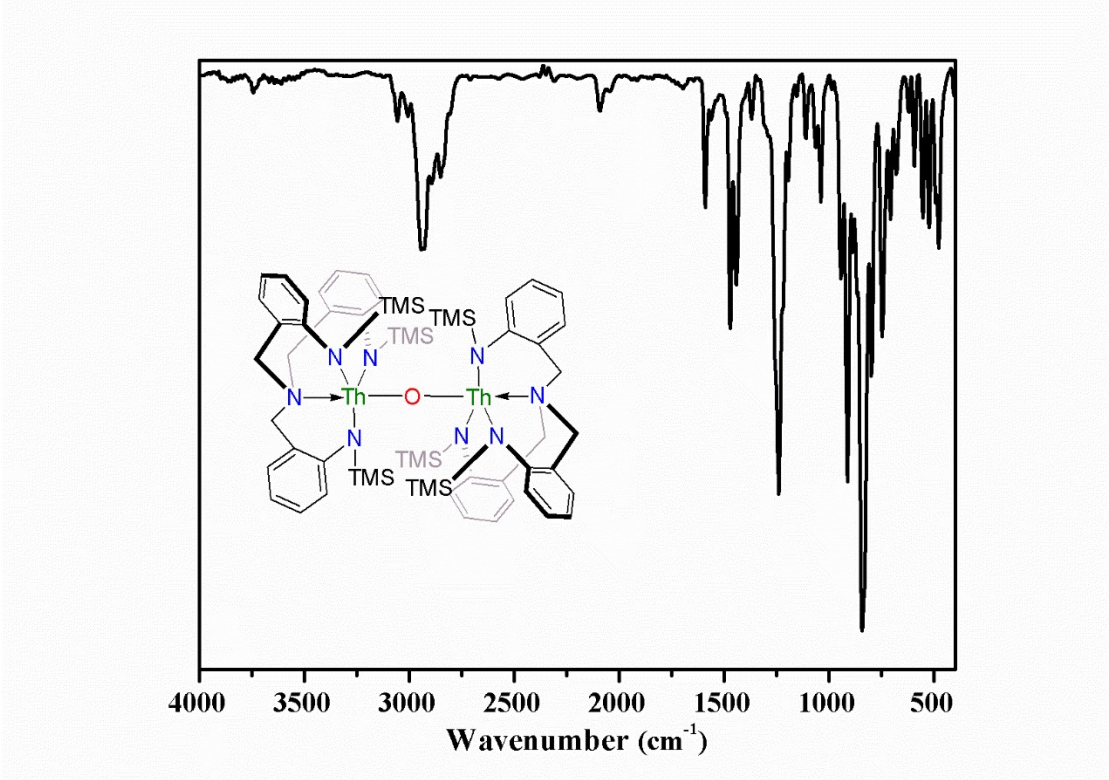

Figure S11. IR spectrum of Complex **3**.

UV-Vis spectrum

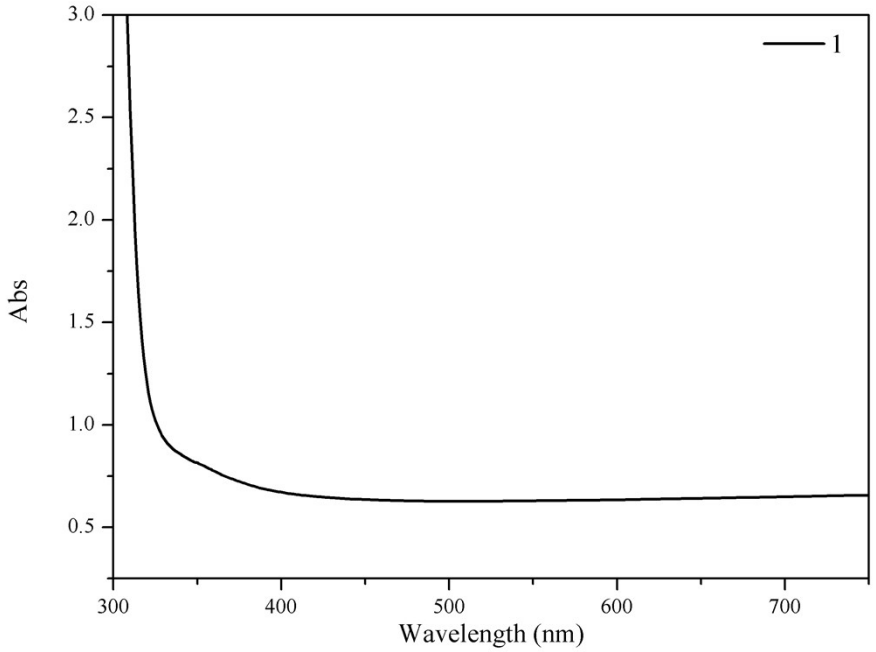

Figure S12. UV-Vis spectrum of Complex **1** in THF at 298 K.

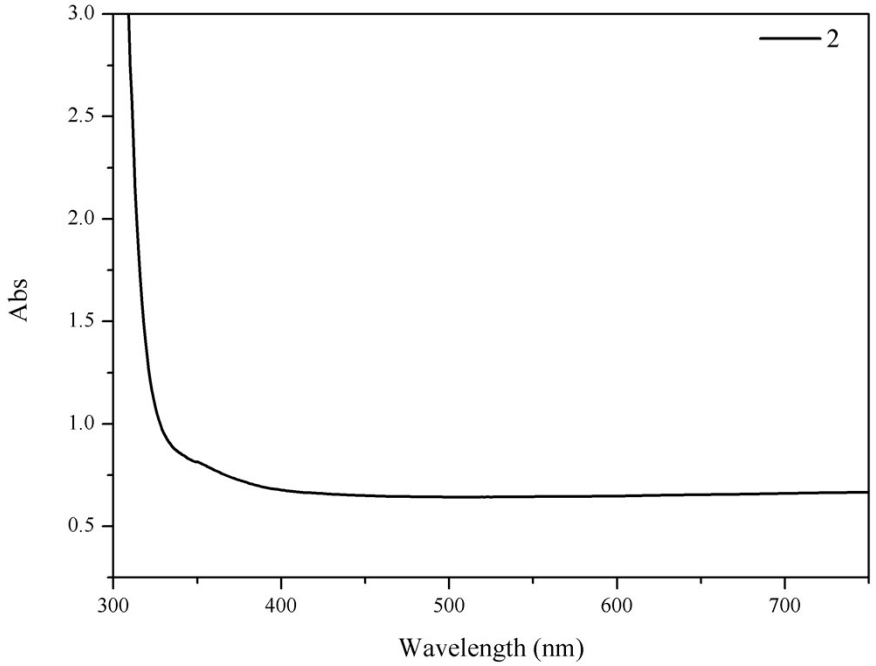

Figure S13. UV-Vis spectrum of Complex **2** in THF at 298 K.

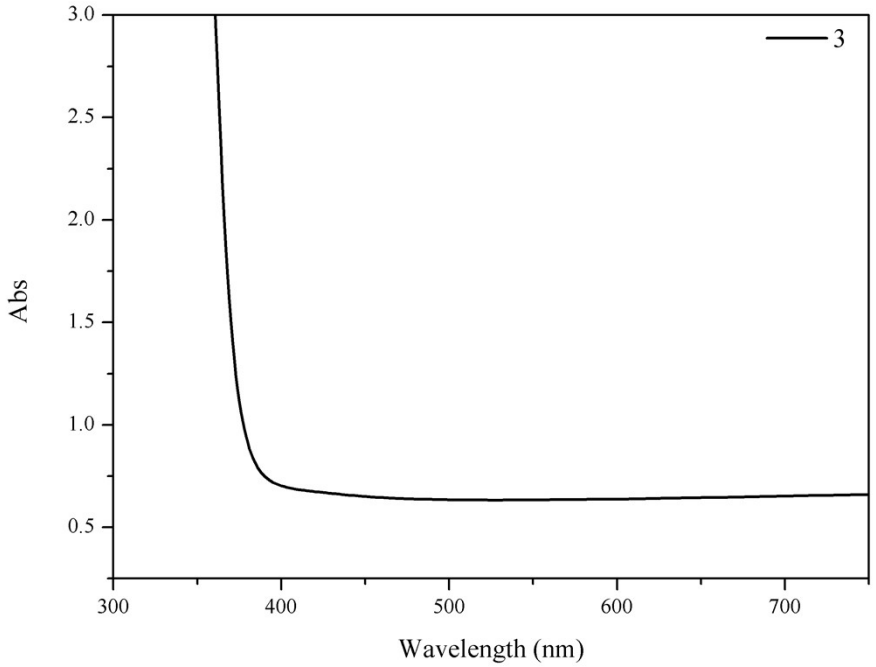

Figure S14. UV-Vis spectrum of Complex **3** in THF at 298 K.

Electrochemistry

Cyclic voltammetry (CV) experiments were performed with an electrochemical workstation (Autolab PGSTAT302N-Metrohm). The data were recorded using Autolab NOVA software (version 1.11) and processed with the same software. The CV experiments were performed in a glovebox under an argon atmosphere. The setup comprised a 4 mL vial, equipped with a CHI 104 glassy-carbon-disk working electrode (CH Instruments, Inc.), a platinum-wire counter electrode and a Ag/AgCl quasi reference electrode. The surface of the working electrode was polished prior to the measurement. THF solutions containing ca. 0.05 mM for **1**, **2** and **3**, and 0.1 M [^{n}Bu$_4$N][PF$_6$] supporting electrolyte were used for the electrochemical analyses. The scan-rate-dependent background of the electrolyte was recorded for each measurement and subtracted from the analyte data. Potentials are referenced to the Fc/Fc$^+$ redox couple used as an internal standard.

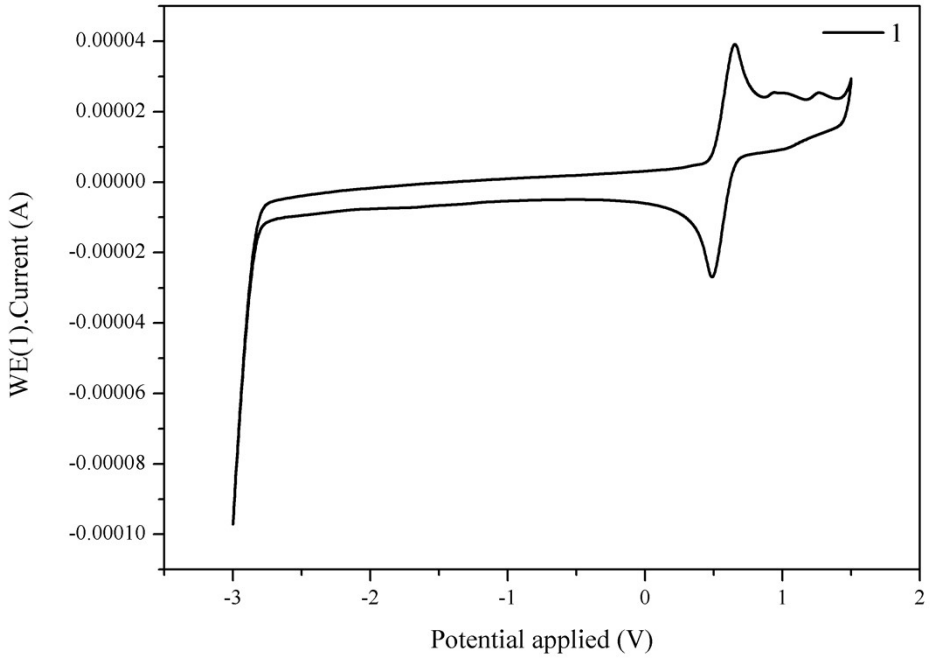

Figure S15. Cyclic voltammograms of Complex **1** in THF (v = 50 mV s^{-1}; c(analyte) = 0.05 mM; c([^{n}Bu$_4$NPF$_6$]) = 0.1 M).

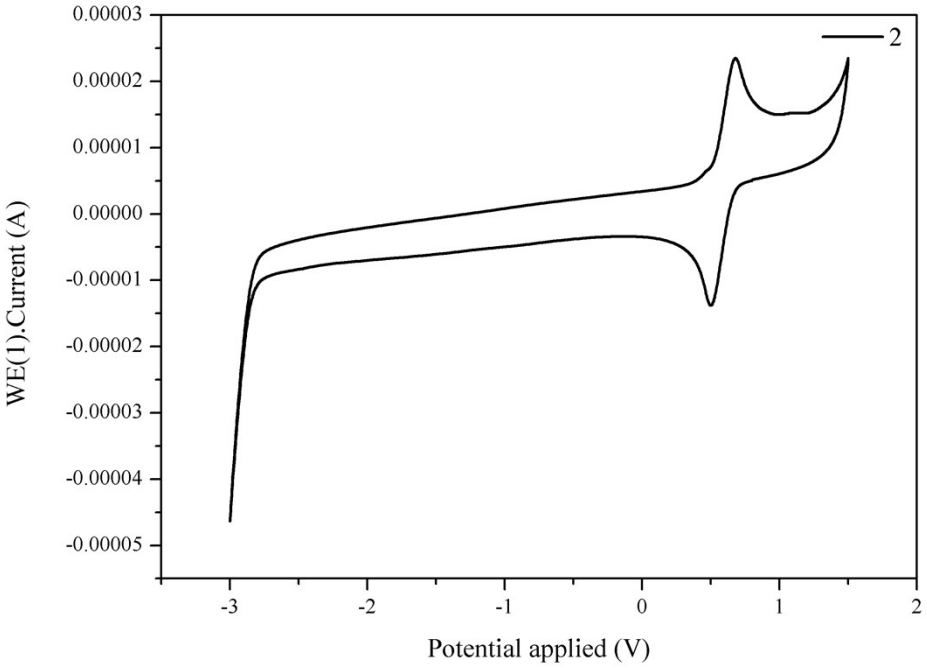

Figure S16. Cyclic voltammograms of Complex **2** in THF (v = 50 mV s^{-1}; c(analyte) = 0.05 mM; c([^{n}Bu$_4$NPF$_6$]) = 0.1 M).

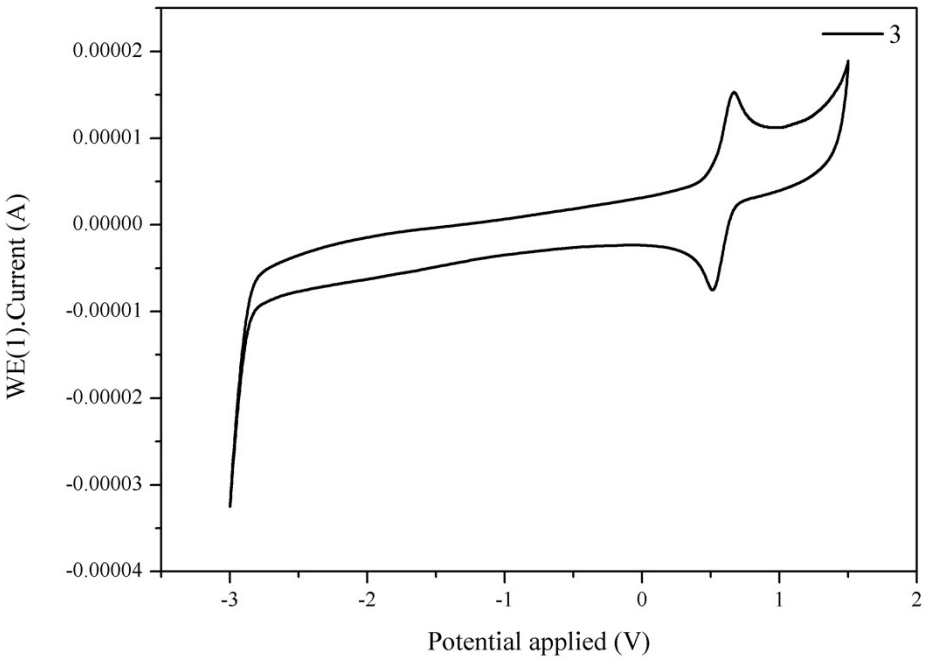

Figure S17. Cyclic voltammograms of Complex **3** in THF (v = 50 mV s^{-1}; c(analyte) = 0.05 mM; c([^{n}Bu$_4$NPF$_6$]) = 0.1 M).

Crystallographic data for 3

Complex Identification code	**3**
Empirical formula	$C_{74}H_{107}N_9Si_6Th_2O_{0.5}$
Formula weight	1763.30
Temperature/K	170.0
Wavelength/Å	0.71073
Crystal system	monoclinic
Space group	$P2_1/c$
Unit cell dimensions	a = 15.0299(8) Å b = 11.9320(6) Å c = 22.0434(10) Å α = 90° β = 94.794(2)° γ = 90°
Volume/Å^3	3939.4(3)
Z	2
Density (calculated)/g/cm^3	1.487
Absorption coefficient/mm^{-1}	3.908
F(000)	1764.0
Crystal size/mm^3	0.13×0.1×0.1
Theta range for data collection	5.58 to 55.022°
Index ranges	-19 ≤ h ≤ 19 -15 ≤ k ≤ 15 -28 ≤ l ≤ 28
Reflections collected	73838
Independent reflections	9048 [R_{int} = 0.1019, R_{sigma} = 0.0488]
Data/restraints/parameters	9048/415/422

Goodness-of-fit on F^2	1.055
Final R indexes [I>=2σ (I)]	R_1 = 0.0356
	wR_2 = 0.0601
Final R indexes [all data]	R_1 = 0.0551
	wR_2 = 0.0645
Largest diff. peak/hole / e $Å^{-3}$	1.19/-1.80

Table S1. Bond lengths [Å] for complex **3**

Atom	Atom	Length/Å	Atom	Atom	Length/Å
Th1	N4	2.801(3)	Si1	C8	1.871(5)
Th1	O1	2.27129(19)	C12	C17	1.405(6)
Th1	N3	2.340(3)	C12	C13	1.399(6)
Th1	N2	2.327(3)	N3	C27	1.427(6)
Th1	N1	2.331(3)	C27	C26	1.404(6)
C1	N4	1.487(5)	C27	C22	1.404(6)
C1	C2	1.500(6)	C16	C17	1.406(6)
N4	C21	1.493(5)	C16	C15	1.381(6)
N4	C11	1.495(5)	N2	C17	1.424(5)
Si2	N2	1.729(4)	N1	C3	1.423(5)
Si2	C20	1.871(5)	C26	C25	1.380(7)
Si2	C19	1.868(5)	C13	C14	1.384(7)
Si2	C18	1.867(5)	C2	C7	1.395(6)
C21	C22	1.510(6)	C2	C3	1.409(6)
Si3	N3	1.741(4)	C22	C23	1.391(6)
Si3	C29	1.866(5)	C23	C24	1.385(7)
Si3	C28	1.864(5)	C24	C25	1.392(8)
Si3	C30	1.863(5)	C7	C6	1.386(7)
C11	C12	1.508(6)	C15	C14	1.374(8)
Si1	N1	1.731(4)	C5	C4	1.384(6)

Si1	C9	1.865(5)	C5	C6	1.377(7)
Si1	C10	1.864(5)	C4	C3	1.406(6)
C32	C31	1.369(11)	C34	C35	1.384(11)
C32	C33	1.280(10)	C34	C33	1.390(11)
C31	C37	1.521(11)	C35	C36	1.453(11)
C31	C36	1.437(11)			

Table S2. Bond angles [°] for complex **3**

Atom	Atom	Atom	Angle/°	Atom	Atom	Atom	Angle/°
O1	Th1	N4	178.22(7)	C17	C12	C13	120.4(4)
O1	Th1	N3	105.05(9)	C13	C12	C11	119.3(4)
O1	Th1	N2	102.15(9)	Si3	N3	Th1	126.41(19)
O1	Th1	N1	104.39(9)	C27	N3	Th1	116.5(3)
N3	Th1	N4	75.58(11)	C27	N3	Si3	116.6(3)
N2	Th1	N4	76.12(11)	C26	C27	N3	121.1(4)
N2	Th1	N3	118.33(12)	C26	C27	C22	118.1(4)
N2	Th1	N1	112.93(12)	C22	C27	N3	120.8(4)
N1	Th1	N4	76.80(11)	C15	C16	C17	120.9(5)
N1	Th1	N3	112.08(12)	Si2	N2	Th1	128.68(18)
N4	C1	C2	114.1(3)	C17	N2	Th1	111.7(2)
C1	N4	Th1	109.7(2)	C17	N2	Si2	119.5(3)
C1	N4	C11	108.4(3)	C12	C17	C16	118.4(4)
C21	N4	Th1	109.4(3)	C12	C17	N2	120.5(4)
C21	N4	C1	111.2(2)	C16	C17	N2	121.0(4)
C21	N4	C11	107.9(3)	Si1	N1	Th1	124.56(18)
C11	N4	Th1	110.2(2)	C3	N1	Th1	115.4(2)
N2	Si2	C20	112.8(2)	C3	N1	Si1	119.9(3)
N2	Si2	C19	106.0(2)	C25	C26	C27	121.4(5)
N2	Si2	C18	113.2(2)	C14	C13	C12	121.2(5)

C19	Si2	C20	107.6(2)	C7	C2	C1	119.8(4)
C19	Si2	C18	106.4(2)	C7	C2	C3	119.6(4)
C18	Si2	C20	110.8(2)	C3	C2	C1	120.5(4)
Th1	O1	Th1[1]	180.0(15)	C27	C22	C21	120.1(4)
N4	C21	C22	112.9(3)	C23	C22	C21	120.0(4)
N3	Si3	C29	113.0(2)	C23	C22	C27	119.9(4)
N3	Si3	C28	112.1(2)	C22	C23	C24	121.3(5)
N3	Si3	C30	107.1(2)	C25	C24	C23	119.1(5)
C29	Si3	C28	106.6(2)	C6	C7	C2	121.4(5)
C29	Si3	C30	109.2(2)	C16	C15	C14	120.7(5)
C30	Si3	C28	108.7(2)	C4	C5	C6	120.8(5)
N4	C11	C12	111.9(3)	C5	C4	C3	121.1(5)
N1	Si1	C9	111.3(2)	C7	C6	C5	119.1(5)
N1	Si1	C10	114.7(2)	C2	C3	N1	120.9(4)
N1	Si1	C8	106.3(2)	C4	C3	N1	121.1(4)
C9	Si1	C10	108.8(2)	C4	C3	C2	118.0(4)
C9	Si1	C8	106.8(2)	C13	C14	C15	119.4(5)
C10	Si1	C8	108.9(2)	C26	C25	C24	120.1(5)
C17	C12	C11	120.2(4)	C35	C34	C33	125.4(9)
C33	C32	C31	125.1(10)	C34	C35	C36	115.9(8)
C32	C31	C37	122.6(9)	C32	C33	C34	117.0(10)
C32	C31	C36	120.1(8)	C31	C36	C35	116.5(8)
C36	C31	C37	117.1(9)				

Calculation studies

Computation method:

The structures of complexes **2** and **3** were optimized by the DFT method with the BP86 functional using the Gaussian 16 program package[1]. The scalar-relativistic small-core pseudopotential ECP60MWB[2, 3] and the corresponding segmented valence basis sets were applied for the Th atom, and the 6-31G(d) basis set was used for H, C, N, O, Si. Wiberg bond indices (WBIs)[4], and localized molecular orbitals (LMO)[5] were analyzed by using Multiwfn 3.8 software[8].

Table S3. The Bond distances (Å) obtained from experimental and theoretical calculations.

complexes	bonds	experiment	calculated
2	Th1-N5	2.555	2.538
	Th1-N7A	2.576	2.615
	Th1-N4	2.669	2.753
	Th1-N1	2.315	2.332
	Th1-N2	2.299	2.315
	Th1-N3	2.309	2.359
	Th1-N1A	2.28	2.316
	Th1-N2A	2.34	2.359
	Th1-N3A	2.33	2.331

	Th1-N5A	2.557	2.616
	Th1-N7	2.48	2.538
3	Th1-N4	2.798	2.842
	Th1-O1	2.2714	2.197
	Th1-N1	2.344	2.354
	Th1-N2	2.324	2.354
	Th1-N3	2.332	2.354

Table S4. The values of WBIs at the BP86/ECP/6-31G(d) level of theory.

complexes	WBIs		
2	Th1-N5	Th1-N7A	Th1-N4
	0.883	0.786	0.555
	Th1-N1	Th1-N2	Th1-N3
	1.285	1.339	1.325
	Th1-N1A	Th1-N2A	Th1-N3A
	1.340	1.287	1.321
	Th1-N5A	Th1-N7	
	0.785	0.882	
3	Th1-N4	Th1-O1	Th1-N3
	0.510	1.580	1.281
	Th1-N2	Th1-N1	
	1.281	1.281	

Table S5. The WBIs of the Th-N and Th-O bonds in complexes **2** and **3** were calculated with Multiwfn software program.

complexes	WBIs		
2	Th1-N5	Th1-N7A	Th1-N4
	0.883	0.786	0.555
	Th1-N1	Th1-N2	Th1-N3
	1.285	1.339	1.325
	Th1-N1A	Th1-N2A	Th1-N3A

	1.340	1.287	1.321
	Th1-N5A	Th1-N7	
	0.785	0.882	
3	Th1-N4	Th1-O1	Th1-N3
	0.510	1.580	1.281
	Th1-N2	Th1-N1	
	1.281	1.281	

Table S6. The MBOs of the Th-N and Th-O bonds in complexes **2** and **3** were calculated with Multiwfn software program.

Complexes	MBOs		
2	Th1-N5	Th1A-N7	Th1A-N4
	0.364	0.312	0.293
	Th1-N1	Th1-N2	Th1-N3
	0.771	0.805	0.779
	Th1-N1A	Th1-N2A	Th1A-N3B
	0.804	0.772	0.777
	Th1-N5A	Th1-N7	
	0.312	0.362	
3	Th1-N4	Th1-O1	Th1-N3
	0.276	0.990	0.790
	Th1-N2	Th1-N1	
	0.791	0.790	

Table S7. The WBIs of the Th-N and Th-O bonds in complexes **2** and **3** were calculated using Gaussian software program at the BP86/ECP60MWB/6-31G(d) theoretical levels.

Complexes	WBIs		
2	Th1-N5	Th1A-N7	Th1A-N4
	0.458	0.424	0.229
	Th1-N1	Th1-N2	Th1-N3
	0.630	0.666	0.661
	Th1-N1A	Th1-N2A	Th1A-N3B
	0.460	0.425	0.230
	Th1-N5A	Th1-N7	
	0.632	0.667	
3	Th1-N4	Th1-O1	Th1-N3
	0.183	0.763	0.587
	Th1-N2	Th1-N1	
	0.587	0.587	

Table S8. The MBOs of the Th-N and Th-O bonds in complexes **2** and **3** were calculated using Gaussian software program at the BP86/ECP60MWB/6-31G(d) theoretical levels.

Complexes	MBOs		
2	Th1-N5	Th1A-N7	Th1A-N4
	0.364	0.312	0.294

	Th1-N1	Th1-N2	Th1-N3
	0.771	0.805	0.779
	Th1-N1A	Th1-N2A	Th1A-N3B
	0.362	0.312	0.294
	Th1-N5A	Th1-N7	
	0.777	0.804	
3	Th1-N4	Th1-O1	Th1-N3
	0.276	0.989	0.790
	Th1-N2	Th1-N1	
	0.790	0.791	

Table S9. The WBIs of the Th-N and Th-O bonds in complexes **2** and **3** were calculated using Gaussian software program at the B3LYP/ECP60MWB/6-31G(d) theoretical levels.

Complexes	WBIs		
2	Th1-N5	Th1A-N7	Th1A-N4
	0.428	0.400	0.211
	Th1-N1	Th1-N2	Th1-N3
	0.586	0.623	0.618
	Th1-N1A	Th1-N2A	Th1A-N3B
	0.430	0.400	0.211
	Th1-N5A	Th1-N7	
	0.617	0.624	

3	Th1-N4	Th1-O1	Th1-N3
	0.165	0.714	0.546
	Th1-N2	Th1-N1	
	0.546	0.546	

Table S10. The MBOs of the Th-N and Th-O bonds in complexes **2** and **3** were calculated using Gaussian software program at the B3LYP/ECP60MWB/6-31G(d) theoretical levels.

Complexes	MBOs		
2	Th1-N5	Th1A-N7	Th1A-N4
	0.318	0.271	0.258
	Th1-N1	Th1-N2	Th1-N3
	0.730	0.767	0.740
	Th1-N1A	Th1-N2A	Th1A-N3B
	0.317	0.272	0.258
	Th1-N5A	Th1-N7	
	0.730	0.768	
3	Th1-N4	Th1-O1	Th1-N3
	0.238	0.935	0.749
	Th1-N2	Th1-N1	
	0.749	0.749	

Table S11. Composition of metal-ligand bonds in complexes **2** and **3** calculated at the BP86/ECP/6-31G(d) level of theory.

Complexes	Bond type	Element	Contributions of each atomic orbital (%)
2	σ	Th1	7s(1.31)6d(0.86)
		N5	2s(82.02)2p(9.96)
	σ	Th1	7s(0.86)6d(0.55)
		N7A	2s(84.59)2p(8.66)
	σ	Th1	7s(2.22)6d(1.04)
		N4	2s(48.63)2p(36.15)
	σ	Th1	7s(4.30)6d(2.46)
		N1	2s(67.05)2p(17.74)
	σ	Th1	7s(4.46)6d(2.87)
		N2	2s(62.25)2p(21.46)
	σ	Th1	7s(4.43)6d(2.58)
		N3	2s(67.89)2p(17.21)
	σ	Th1	7s(4.46)6d(2.87)
		N1A	2s(62.25)2p(21.46)
	σ	Th1	7s(4.30)6d(2.47)
		N2A	2s(67.14)2p(17.66)
	σ	Th1	7s(4.45)6d(2.58)
		N3A	2s(67.81)2p(17.26)
	σ	Th1	7s(0.85)6d(0.55)

		N5A	2s(84.66)2p(8.59)
	σ	Th1	7s(1.31)6d(0.86)
		N7	2s(82.00)2p(10.04)
3	σ	Th1	7s(1.48)6d(0.54)7p(0.63)
		N4	2s(48.86)2p(36.29)
		Th1	7s(5.88)6d(3.73)5f(1.34)
	σ	Th1	7s(5.88)6d(3.73)5f(1.34)
		O1	2p(70.70)
		Th1	6d(2.91)5f(0.50)
	π	Th1	6d(2.91)
		O1	2p(87.15)
		Th1	6d(2.91)
	π	Th1	6d(2.91)
		O1	2p(87.14)
	σ	Th1	7s(4.95)6d(2.51)
		N3	2s(66.50)2p(18.23)
	σ	Th1	s(4.95)6d(2.51)
		N2	2s(66.49)2p(18.24)
	σ	Th1	s(4.95)6d(2.51)
		N1	2s(66.50)2p(18.23)

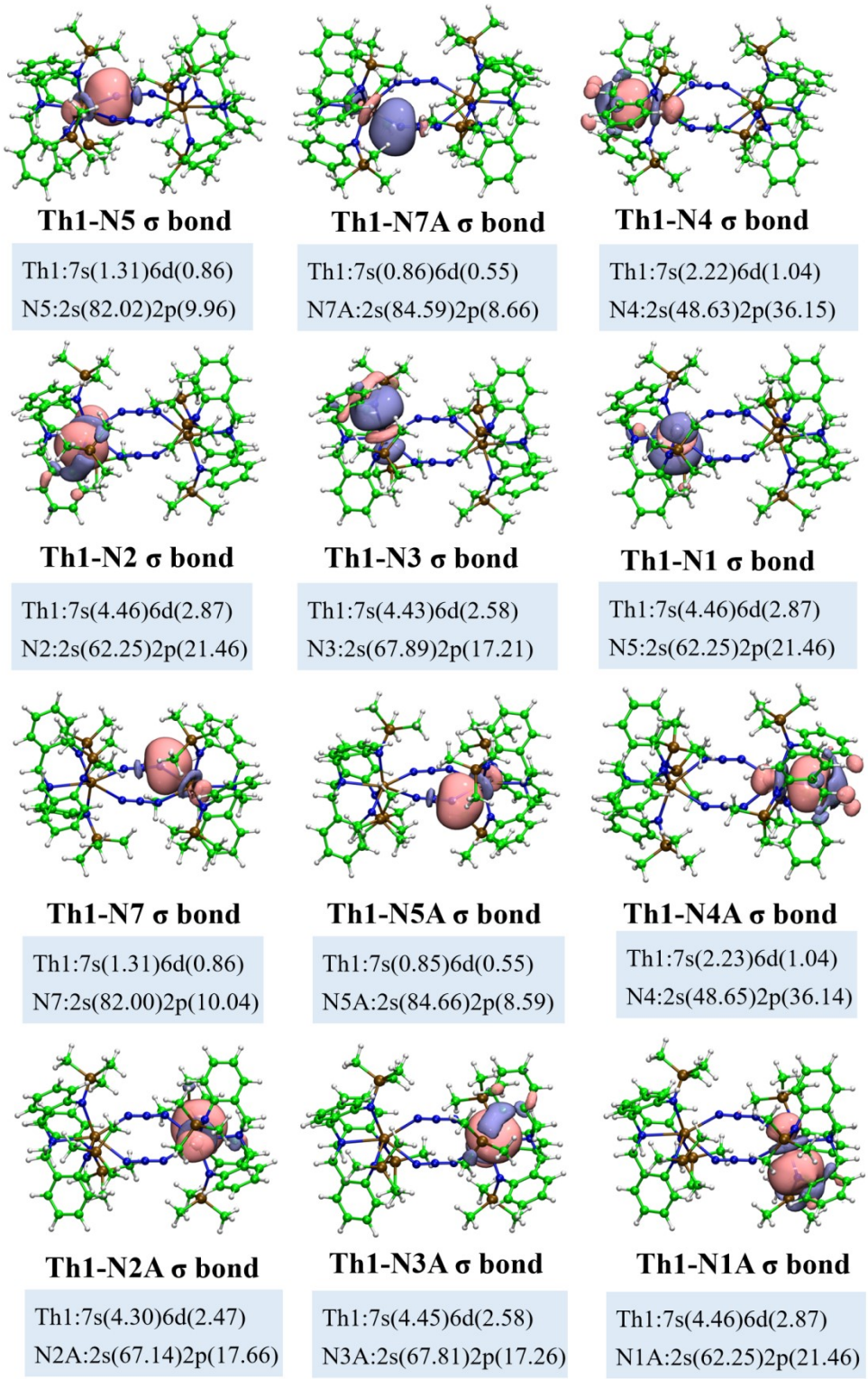

Figure S18. The LMO plots of complex **2** at the BP86/RECP/6-31G(d) level of theory (The isosurface value is set as 0.01 a.u.)

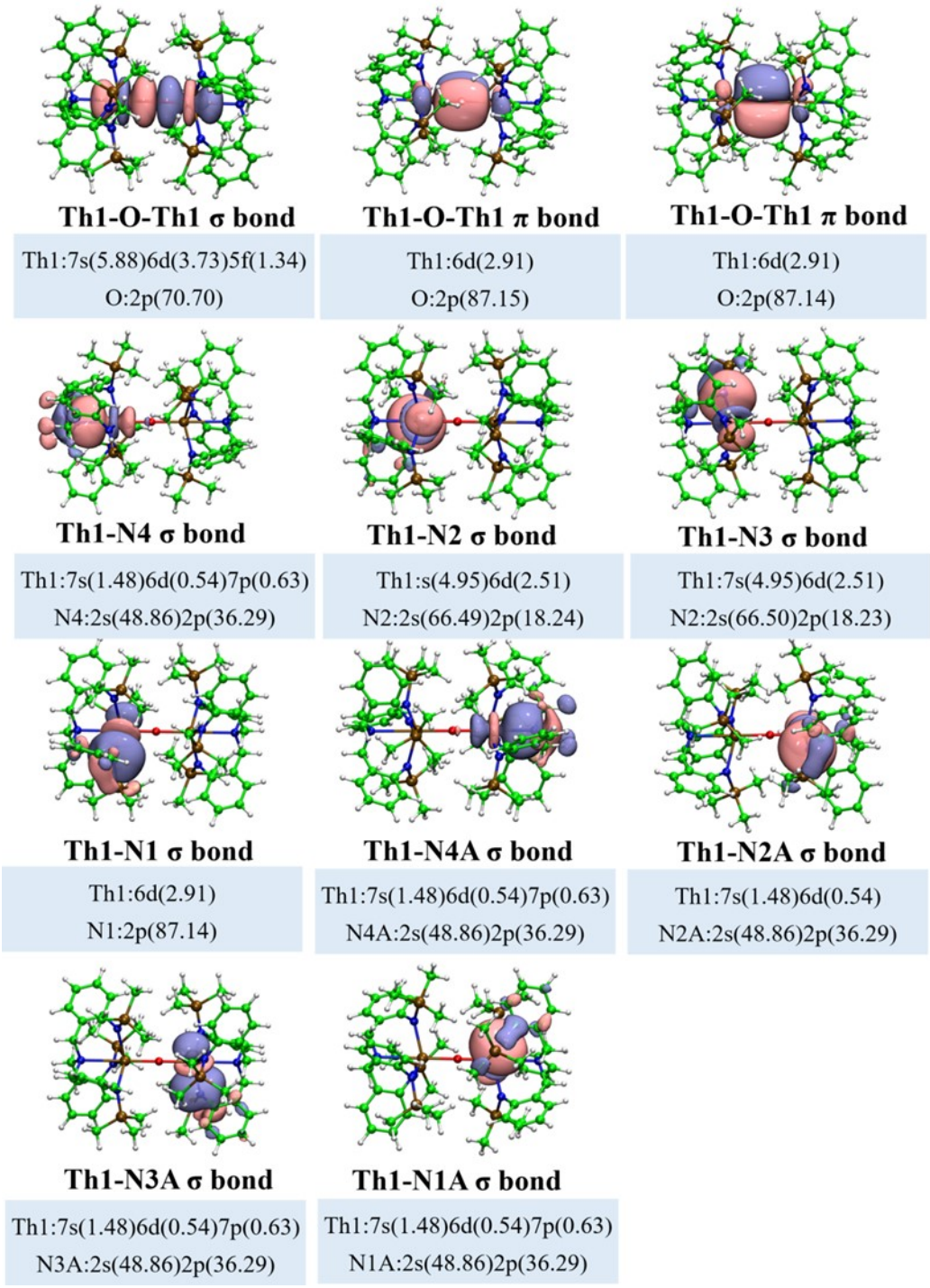

Figure S19. The LMO plots of complex **3** at the BP86/RECP/6-31G(d) level of theory (The isosurface value is set as 0.01 a.u.)

References

(1) Frisch, M. J.; Trucks, G. W.; Schlegel, H. B.; Scuseria, G. E.; Robb, M. A.; Cheeseman, J. R.; Scalmani, G.; Barone, V.; Petersson, G. A.; Nakatsuji, H.; Li, X.; Caricato, M.; Marenich, A. V.; Bloino, J.; Janesko, B. G.; Gomperts, R.; Mennucci, B.; Hratchian, H. P.; Ortiz, J. V.; Izmaylov, A. F.; Sonnenberg, J. L.; Williams-Young, D.; Ding, F.; Lipparini, F.; Egidi, F.; Goings, J.; Peng, B.; Petrone, A.; Henderson, T.; Ranasinghe, D.; Zakrzewski, V. G.; Gao, J.; Rega, N.; Zheng, G.; Liang, W.; Hada, M.; Ehara, M.; Toyota, K.; Fukuda, R.; Hasegawa, J.; Ishida, M.; Nakajima, T.; Honda, Y.; Kitao, O.; Nakai, H.; Vreven, T.; Throssell, K.; Montgomery, J. A., Jr.; Peralta, J. E.; Ogliaro, F.; Bearpark, M. J.; Heyd, J. J.; Brothers, E. N.; Kudin, K. N.; Staroverov, V. N.; Keith, T. A.; Kobayashi, R.; Normand, J.; Raghavachari, K.; Rendell, A. P.; Burant, J. C.; Iyengar, S. S.; Tomasi, J.; Cossi, M.; Millam, J. M.; Klene, M.; Adamo, C.; Cammi, R.; Ochterski, J. W.; Martin, R. L.; Morokuma, K.; Farkas, O.; Foresman, J. B.; Fox, D. J. *Gaussian 16*, revision B; Gaussian, Inc.: Wallingford, CT, **2016.**

(2) Cao, X.; Dolg, M.; Stoll, H. J. J. o. C. P. Valence basis sets for relativistic energy-consistent small-core actinide pseudopotentials. **2001**, *118*, 487-496.

(3) Cao, X.; Dolg, M. Segmented contraction scheme for small-core

actinide pseudopotential basis sets. *J. Mol. Struct.: THEOCHEM.* **2004**, *673*, 203-209.

(4) Wiberg, K. B. Application of the Pople-Snatry-Segal complete neglect of differential overlap method to some hydrocarbons and their cations. *J. Am. Chem. Soc.* **2002**, *90*, 59-63.

(5) Lu, T.; Chen, F. Multiwfn: A multifunctional wavefunction analyzer. *J. Comput. Chem.* **2012**, *33*, 580-592.

(6) Bader, R. F. A quantum theory of molecular structure and its applications. *Chem. Rev.* **1991**, *91*, 893-928.

(7) Bader, R. F. W.; Matta, C. F. Bonding to Titanium. *Inorg. Chem.* **2001**, *40* , 5603-5611.

(8) Lu, T. A comprehensive electron wavefunction analysis toolbox for chemists, Multiwfn. *J. Chem. Phys.* **2024**, *161*, 0802503.